JOURNAL OF APPLIED ELECTROCHEMISTRY 12 (1982) 417–423

Metal deposition in magnetoelectrolysis employing low frequency sine-pulse trains

A. OLIVIER*, T. Z. FAHIDY

Department of Chemical Engineering, University of Waterloo, Waterloo, Ontario, Canada N2L 3G1

Received 2 November 1981

The effect of uniform magnetic fields on the electrolytic deposition of copper in electric fields consisting of a d.c. bias voltage and a superimposed rectified sine-pulse train of 1 mHz–0.1 Hz frequency was investigated in an experimental cell. At appropriate combinations of magnetic flux density and potential frequency, good quality deposits can be obtained at elevated cathode current densities. Current oscillations observed under certain conditions are directly related to strong surface deterioration.

1. Introduction

Metal deposition via pulsating potential and rectified half potential wave electrolysis has recently received a good deal of attention in the literature. Various structural and morphological [1–3], mass transport [4, 5] and modelling [6–8] studies were followed by the investigation of the imposed magnetic field effect on certain aspects of process performance [9]. The latter has shown that certain combinations of magnetic field strength and pulsation frequency result in good quality deposits even at current densities significantly higher than encountered in conventional d.c. deposition processes. These preliminary results clearly indicate the necessity for a comprehensive study of magnetoelectrolysis in pulsed and rectified half-wave electric fields, especially at relatively high potential amplitudes.

The purpose of this paper is to summarize the results of experiments where the potential field imposed at the electrodes consisted of a d.c. bias voltage and a superimposed rectified sine-wave voltage variation: the effect of the d.c. component magnitude and the rectified potential train on the deposition rate and the quality of the deposit at various magnetic field strengths was investigated in order to obtain further quantitative information about the performance of such electrolytic cells. The data obtained may be useful for the design of rectified wave electrolytic metal recovery cells using supportive magnetic fields.

2. Experimental details

The apparatus is similar to that used in earlier investigations [9, 10]. As shown in Fig. 1 the magnetic flux lines are perpendicular to the electric field, which consists of a rectified sine wave train of d.c. component V_c and train amplitude $(V_T - V_c)$, shown in Fig. 2a. The numerical value of V_c was set to 0.6, 1.0 and 1.5 V and V_T was chosen to be sufficiently large to reach beyond the limiting current plateau (Fig. 2b). The train frequency was varied between 1 mHz and 0.1 Hz by means of a programmable function generator – power supply assembly. The magnetic field was generated by a 5 kVA Walker regulated d.c. electromagnet with a residual flux density of 4 mT; at the pole face separation used (about 18 cm) the maximum flux density attainable was 685 mT. The variation of current with imposed potential and time was monitored by a conventional chart recorder of variable speed and amplifier gain settings. The copper electrodes (active area: 3.65 cm^2) were cleaned first mechanically, then washed in water and alcohol, dried and placed in the electrolytic cell containing an aqueous $CuSO_4$/H_2SO_4 solution, for electrolysis. After an experiment, the electrodes were carefully washed and

* Permanent address: Laboratoire d'Electrochimie, Faculté des Sciences, Université de Reims, Moulin de la Housse BP 347, 51062, Reims, France.

0021–891X/82/040417–07$03.34/0

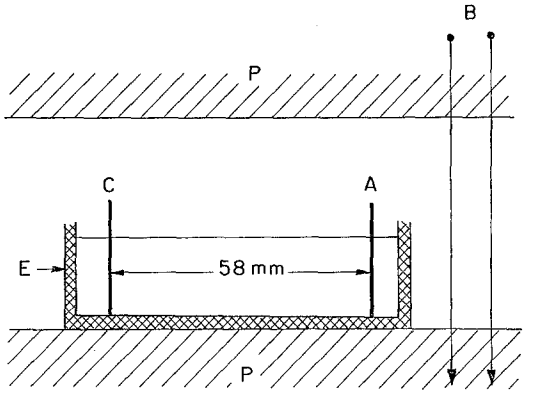

Fig. 1. Sketch of the experimental apparatus. A: anode; B: magnetic flux lines (N → S); C: Cathode; E: electrolytic cell; P: magnetic pole faces.

dried and samples of the fresh deposit appropriately prepared were subjected to examination by an ultramicroscope equipped with a photographic camera.

3. Results and discussion

3.1. *General current and potential behaviour*

In the absence of a magnetic field, and at low potential train frequencies ($f < \sim 0.1$ Hz) the current–potential relationship follows the curve shown in Fig. 2b. The ascending portion of the curve consists of three distinct sections and asymptotes numbered 1–3. They are related to charge transfer, mass transfer and hydrogen evolution control, respectively. Under d.c. conditions and at very low frequencies ($f < 0.01$ Hz) the experimentally measured plateau current (asymptote 2) density agrees reasonably well with theoretical predictions: e.g. in a 0.542 mol dm^{-3} $CuSO_4$–1.605 mol dm^{-3} H_2SO_4 electrolyte the experimental value of $i_L = 592$ A m^{-2} may be compared with the theoretical estimate of 570.5 A m^{-2} based on the bisulphate model of Selman and Newman [11] for natural convection; a faster approximate calculation based on simple classical theory yields a value of 574 A m^{-2}, if the transference number of Cu^{2+} ions is neglected, and 606.2 A m^{-2} if it is estimated to be about 0.054. The intersection of the first and second asymptote defines a potential V_L, falling in the mixed charge transfer/mass transfer control regime. For cycle amplitudes $V_T < V_L$ the cathode deposit is invariably bright and adherent, whereas for $V_T > V_L$ hydrogen evolution at the cathode leads to poor quality deposits after a number of deposition cycles. In this sense, V_L might be regarded as a 'limiting' deposition potential. As shown in Figs 3 and 4, V_L is essentially a linear function of the imposed magnetic field strength within the

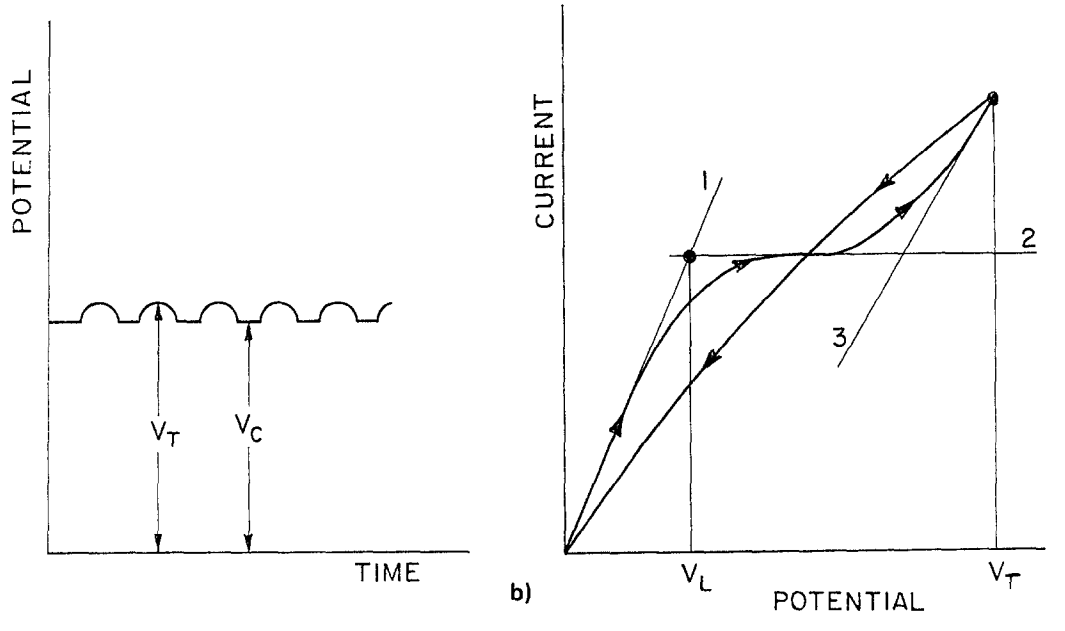

Fig. 2. Imposed potential and a typical current–potential variation during one cycle.

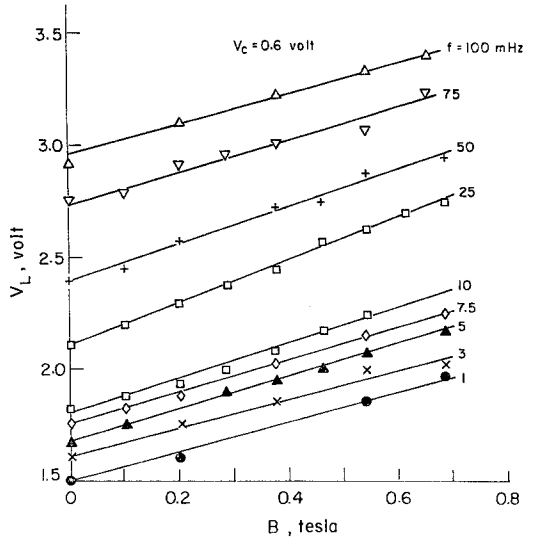

Fig. 3. The variation of V_L with magnetic flux density at various cycle frequencies and at $V_c = 0.6$ V.

range of the experimental potential train frequency; at a fixed value of B, V_L increases with frequency. It follows that good quality cathode deposits can readily be obtained at potentials significantly higher than those associated with d.c. electrolysis, at sufficiently high frequencies and magnetic flux densities. The slope of the $V_L(B)$ line varies between 0.5 and 0.96 V T^{-1} when $V_c = 0.6$ and between 0.64 and 0.99 V T^{-1} when $V_c = 1$. At frequencies higher than about 0.1 Hz, the current plateau in Fig. 2b becomes gradually less distinct and V_L cannot be obtained

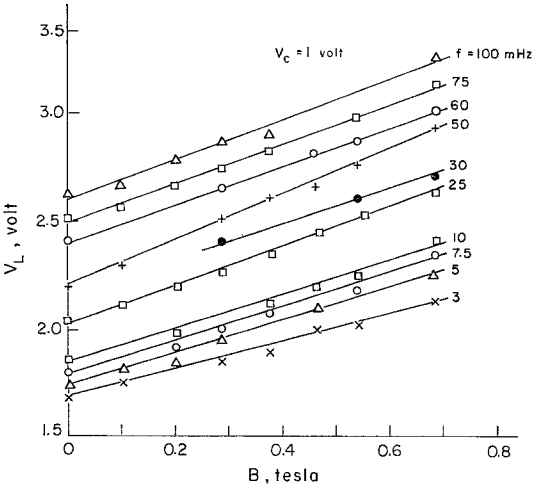

Fig. 4. The variation of V_L with magnetic flux density at various cycle frequences and at $V_c = 1$ V.

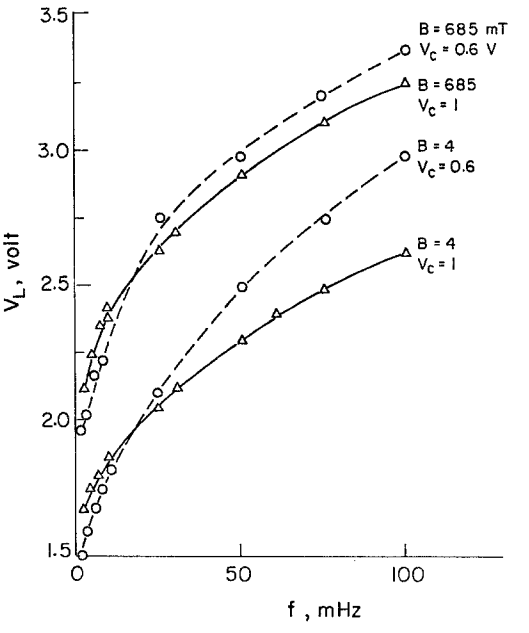

Fig. 5. The variation of V_L with cycle frequency at the lowest and highest experimental magnetic flux density.

with a good degree of accuracy. Similar observations pertain to large values of V_T, where rough and porous cathode deposits accompany the virtual disappearance of the current plateau.

The effect of the imposed magnetic field can be analysed further by plotting V_L against frequency as shown in Fig. 5, and by plotting the cathodic current density against B as shown in Fig. 6. Figure 5 shows clearly that the magnetic

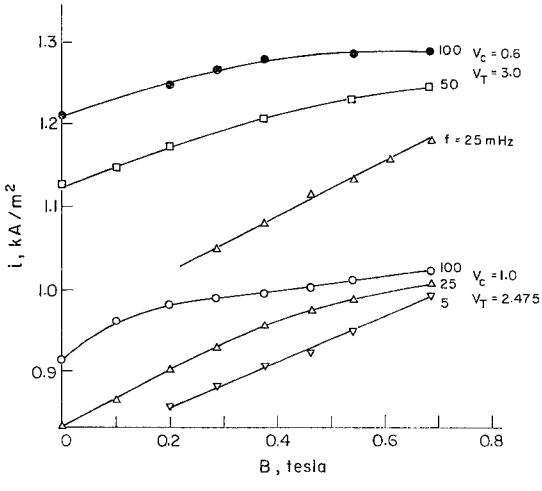

Fig. 6. The effect of the magnetic flux density on experimental observed current densities at various cycle frequencies.

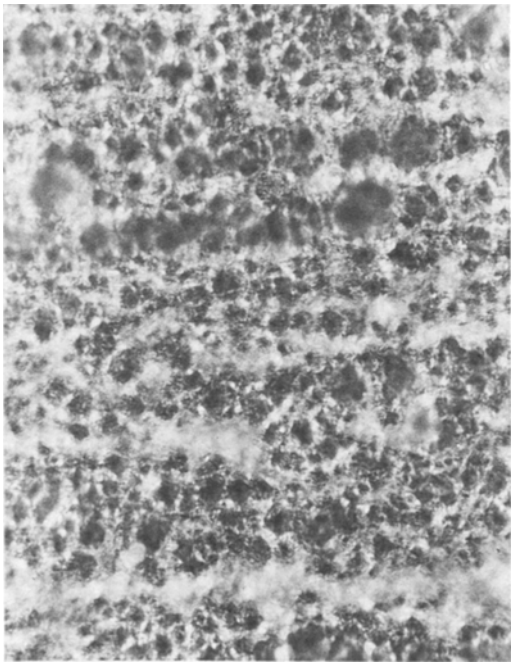

Fig. 7. Typical cathode deposit quality under normal conditions of rectified half-wave electrolysis (magnification $\times 40$; $V_T = 1.96$ V; $f = 3$ mHz; $B = 0.460$ T; the micrograph represents a randomly chosen portion of the highly uniform electrode surface).

field reduces the opposing effect of the d.c. bias potential V_c on the potential region of good quality deposits. In consequence, progressively larger current densities can be attained as the flux density is increased. However, the relative increase (with respect to the residual field strength) becomes less pronounced as the frequency is increased, and as seen in Fig. 6, the magnetic field will exert essentially no further influence past a certain value (see, for example, the uppermost curve corresponding to $f = 0.1$ Hz, at $B > \sim 0.45$ T). This finding is in full agreement with earlier results [10] which indicate such an intricate interaction between potential train frequency and magnetic field strength. In all instances the cathode deposit is of good quality; a typical homogeneous deposition structure is shown in Fig. 7.

3.2. *Oscillatory current behaviour*

In a specific set of experiments V_C was set at less than 100 mV below the value of V_L corresponding to a particular combination of frequency and magnetic field strength. The amplitude of the potential train was carefully chosen such that the $V_T \sim V_L$ condition was maintained. The development of current oscillation with cycle number is illustrated in Fig. 8, composed from current versus time recordings. The first few cycles (not shown) exhibit a perfectly normal current response, but in subsequent cycles the instantaneous current oscillates at increasing amplitudes during the on-half cycle; as time progresses (cycle 7 in Fig. 8) oscillations also appear in the base current (corresponding to V_c). These oscillations gradually disappear as the instantaneous current amplitude becomes smaller and smaller (cycles 9 and 14). As an illustration, at $V_c = 1.5$, $V_T = 2.25$, $f = 3$ mHz and $B = 0.685$ T, the current oscillation frequency is 0.343 Hz during the second cycle and 0.214 Hz in the third cycle; in cycles up to 9, the frequency remains at about 0.17 Hz. Past the ninth cycle only short-term oscillations remain which disappear fully after the thirteenth cycle. The phenomenon is highly reproducible at all potential-train frequencies investigated in the 3 mHz–0.1 Hz range and its development is *accelerated* by the presence of a magnetic field. Micrographs taken of anode surfaces exposed to this mode of electrolysis reveal a characteristic deposit structure illustrated in Fig. 9: the upper portion of the anode plate is covered by large grain-sized oxide growths separated by poor quality surface sections, whereas the lower portion of the plate consists of a smooth, uniformly dissolving copper surface. Notice the position of this portion relative to magneto-hydrodynamic (MHD) force lines, and the higher the magnetic flux density, the *smaller* the size of the lower, high quality anode surface region. Micrographs taken from cathode samples also indicate large grain-sized deposit regions.

Although the oscillatory behaviour described above is not yet fully understood, a qualitative interpretation of the observed phenomena can be advanced in the following manner. Consider the cathode first, in the absence of an imposed magnetic field but at a relatively high value (e.g. 1.5 V) of the d.c. bias potential. Throughout the 'normal' cycles, i.e. where the current response is normal, the cathodic current distribution is slightly nonuniform and the deposit quality is good throughout the cathode surface. On further cycling of the imposed potential the current distribution

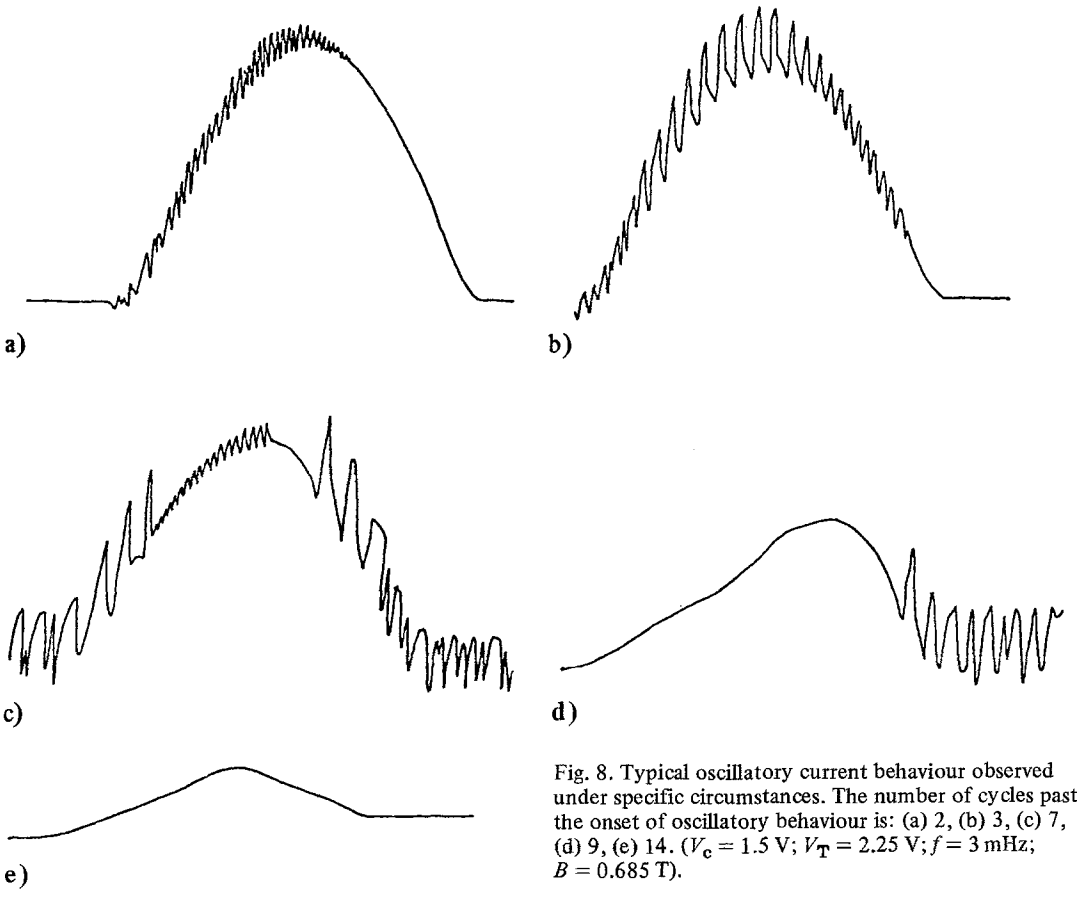

Fig. 8. Typical oscillatory current behaviour observed under specific circumstances. The number of cycles past the onset of oscillatory behaviour is: (a) 2, (b) 3, (c) 7, (d) 9, (e) 14. ($V_c = 1.5$ V; $V_T = 2.25$ V; $f = 3$ mHz; $B = 0.685$ T).

becomes progressively nonuniform and the cathode surface consists increasingly of protrusions (active zones) and interconnecting cavities (inactive zones); this structure is sometimes represented by a sawtooth pattern (e.g. [5]). Due to relatively high local current (densities) at active centres, as the train potential approaches its maximum value V_T, excessive H_2 evolution will cause temporary 'blocking' of the surface with a subsequent drop in current flow and in its proton discharging component. As a result, the blocking gas blanket is released and the current begins to increase, leading to the same blocking process as before. The repetition of the blocking–releasing cycle appears as current oscillation occurring at a frequency characteristic of the process parameters. Further cycling causes a gradual amplification of the oscillatory behaviour, with strong subsequent deterioration of the cathode surface; the oscillation frequency remains essentially the same throughout a number of successive cycles (three to nine under the conditions of Fig. 8). Beyond this stage the deteriorated surface begins to exhibit a high relative resistance to the flow of current, whose amplitude becomes progressively smaller; oscillation finally vanishes as a large proportion of the surface, indicated in Fig. 9, is covered by poor quality deposit. Since Fig. 9 represents *both* anode and cathode at this stage, the development of the anode surface structure is similar; O_2 evolution leads to loss of active areas for anodic copper dissolution and the increasing coverage of copper oxides of the anode surface is probably related to the oscillatory behaviour of the electric current.

The effect of the magnetic field strength on the oscillation phenomenon is more difficult to explain since it cannot be interpreted in terms of (purely) magnetohydrodynamic (MHD) factors: there is no straightforward MHD reason for the accelerating effect of magnetic induction on the development of oscillation. Although there exists no *prima facie* evidence for the magnetic field effect to be restricted to the anode or to the cathode exclusively, it appears more likely that the magnetic field inter-

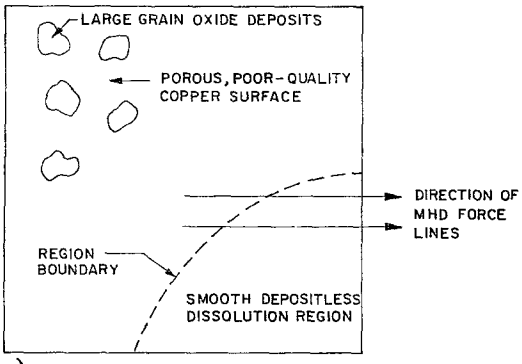

a)

b)

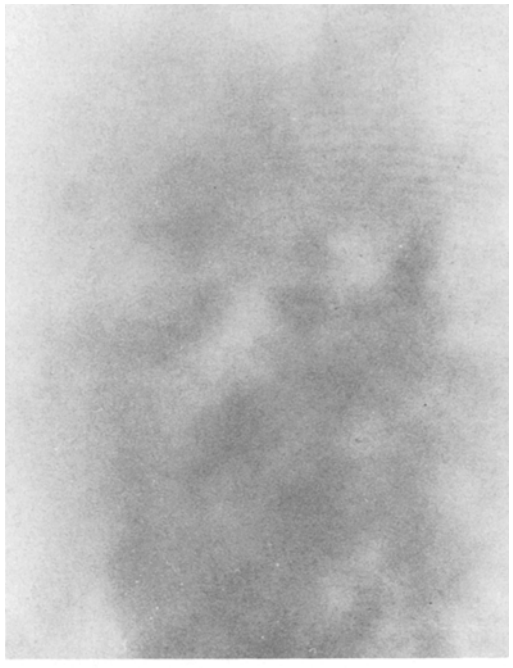

c)

Fig. 9. The structure of a typical anode surface in the wake of oscillatory current behaviour: (a) overall electrode surface; (b) micrograph of the oxide deposit (upper left portion); (c) micrograph of the dissolution region (lower right portion).

action is manifest in one (or more) of the following anode processes [12–14]: Copper dissolution and disproportionation:

$$Cu \rightarrow Cu^{+} + e^{-} \quad (1)$$

$$Cu \rightarrow Cu^{2+} + 2e^{-} \quad (2)$$

$$2Cu^{+} \rightarrow Cu + Cu^{2+}. \quad (3)$$

O_2 evolution at high current density and in the presence of (strong) sulphuric acid:

$$2H_2O \rightarrow O_2 + 4H^{+} + 4e^{-} \quad (4)$$

$$2SO_4^{2-} \rightarrow 2SO_3^{\cdot} + O_2 + 4e^{-} \quad (5)$$

$$2SO_3^{\cdot} + 2H_2O \rightarrow 2SO_4^{2-} + 4H^{+}. \quad (6)$$

Since Equation 3 results in a powdery copper deposition which in turn helps the surface deterioration process, and since the velocity of Equations 5 and 6 determines the rate of oxygen evolution, hence the rate of surface deterioration by direct oxidation, the magnetic field effect might be attributable to its acceleration of the kinetics of Equations 3 and/or 5 and 6. A variation of the theme, acceleration of the formation kinetics of the $H_2S_2O_8$ and HSO_5 species [15], or interaction with the process [16]

$$2Cu^{+} + \tfrac{1}{2}O_2 \rightarrow 2Cu^{2+} + O^{2-} \quad (7)$$

where the O^{2-} species is bounded to a metal ion on the oxide surface, may also be considered. It appears that conditions engendering oscillatory current behaviour are established only at a sufficiently high d.c. bias potential; when V_c is low (in the experimental work, less than 1.5 V) the potential train imposes amplitudes of insufficient time length to cause surface deterioration. The

higher the cycle frequency the higher the potential train amplitude the electrodes can endure. If V_c is higher than a particular threshold value, surface deterioriation is induced by the continuous d.c. potential and the potential train acts as an enhancing agent of the deterioration process. The exact understanding of the interaction of the magnetic field with this phenomenon will require substantially more work and is well beyond the scope of this paper.

4. Concluding remarks

The foregoing results provide a further demonstration of the complex relationship between potential train amplitude and frequency, magnetic field strength and d.c. bias potential, which determines the quality of cathode deposits in pulse train electrolysis. Oscillatory current behaviour suggests periodic surface processes accompanying electrode deterioration and possible interactions of the imposed magnetic field with pertinent reaction mechanisms. Further technological and theoretical aspects of potential train electrolysis will have to be studied for a comprehensive understanding of all important phenomena involved.

Acknowledgement

This project was supported by the Natural Sciences and Engineering Research Council of Canada and the Canada–France Exchange of Scientists Programme.

References

[1] A. R. Despić and K. I. Popov, *J. Appl. Electrochem.* **1** (1971) 275.
[2] K. I. Popov, D. N. Keča and M. D. Andjelić, *J. Appl. Electrochem.* **9** (1978) 19.
[3] N. Ibl, J. C. Puippe and H. Angerer, *Surface Technology* **6** (1978) 287.
[4] N. Ibl. *Metalloberfläche* **33** (1979) 51.
[5] J. C. Puippe, R. Frey and N. Ibl, *Oberfläche-Surface* **19** (1978) 298.
[6] K. I. Popov, D. N. Keča, S. I. Vidojković, B. J. Lazarević and V. B. Milojković, *J. Appl. Electrochem.* **6** (1976) 365.
[7] K. Viswanathan, H. Y. Cheh and G. L. Standart, *J. Appl. Electrochem.* **10** (1980) 37.
[8] K. Viswanathan and H. Y. Cheh, *J. Appl. Electrochem.* **9** (1979) 29.
[9] M. S. Quraishi, T. Z. Fahidy and M. S. E. Abdo, *Electrochim. Acta.* in press.
[10] M. S. E. Abdo, M. S. Quraishi and T. Z. Fahidy, *Proc. 2nd World Congress of Chemical Engineering*, Vol. III, Montreal, Canada 4–9 Oct. (1981) Canadian Society for Chemical Engineering, Ottawa. p. 214–6.
[11] J. R. Selman and J. Newman, *J. Electrochem. Soc.* **118** (1971) 1070.
[12] L. I. Antropov, 'Theoretical Electrochemistry', 2nd edn, Nauka, Moscow (1969).
[13] M. A. Gerovich and R. I. Kaganovich, *Trud. Chetv. Sovesh. po Elektrokhim.* 1–6 Oct. Moscow (1956) (edited by A. N. Frumkin *et al.*) p. 277.
[14] M. A. Gerovich, R. I. Kaganovich, V. A. Vergelesov and L. N. Gorokhov, *Dokl. Akad. Nauk SSSR* **114** (1957) 1049.
[15] J. Koryta, J. Dvořák and V. Bohácková, 'Electrochemistry', Methuen, London (1970).
[16] A. Damjanovich and A. T. Ward, 'The Mechanism of Growth of Thin Anodic Oxide Films, Physical Chemistry', Series Two, Vol. 6, 'Electrochemistry, International Review of Science' (edited by A. D. Buckingham and J. O'. M. Bockris) Butterworths, Borough Green (1976).